

LINEAR AND NON-LINEAR IMAGE PROCESSING OPERATIONS ON DIGITAL PROJECTIONS

I. SVALBE

*Centre for X-Ray Physics and Imaging
School of Physics and Materials Engineering
Monash University
Melbourne Australia 3800*

Abstract This paper outlines methods to perform basic spatial operations on 2D digital images that have been mapped into an equivalent set of digital projections. The digital projections are generated using the Discrete Radon Transform (DRT). Each digital projection is similar to an oriented straight-line integral of the Radon transform and the set of digital projections resembles the sinogram from classical tomography. Mapping discrete 2D data to a set of discrete 1D projections provides representational advantages and significant computational efficiency for some operations. The 2D distribution of image pixels viewed along each direction is expressed through one 1D digital projection. The integration of image values to form a directed projection smooths and hence compresses the variance of the original data. The DRT may, however, complicate the comparison of individual pixel values across a local area of the image, because it stores values that are global sums of local intensities. Pixel locations across a region of interest can be linked to those digital projections that contain contributions from those local values. Groups of pixels can be selected by particular translations of digital rays to form periodic lines. Algorithms for generalized linear convolution operations in the DRT domain are presented, as is an initial review of the effect of non-linear, rank-based operators applied to digital projections in the DRT space.

Keywords: Discrete geometry, digital projection, discrete Radon transform.

1. Introduction

A well-developed set of linear and nonlinear algorithms is available to process the image information in the spatial domain. Mapping data from the spatial domain to another representation, such as the Fourier domain, emphasizes certain aspects of the data. For example, the Fourier transformation highlights periodic structures. Spatial operations produce an equivalent mapped result

for the processed image in the transform domain. If the mapping is a 1:1 transformation, then either representational domain is equivalent. The design of processing algorithms for any given operation is generally more efficient or flexible using one domain, rather than the other.

Here the interest is in mapping discrete image data to form a set of discrete, oriented projections and being able to interpret and manipulate the projection data. One objective is to perform image matching by comparing projected image data sets rather than spatial image data. A comparison of filtered projection data avoids the need to project and reconstruct images in order to perform spatial domain comparisons. Projection and reconstruction processes are computationally demanding as they map N by N data points using order N operations per point.

The Discrete Radon Transform (DRT) provides an alternate view of discrete image data, portrayed in the form of digital projections. A digital projection is a sum of pixel values taken at discrete sample intervals along a set of parallel, straight-line rays that are aligned with the locations of the points of a regular lattice. With a representative set of angles, the set of digital projections forms an exact and invertible representation of discrete image data [1]. The aim of this work is to interpret fully the content of digital projections and to be able to manipulate their contents.

The DRT has been applied to perform data compression [1], tomographic reconstruction using real projection data [6, 7] and as a model for the chaotic energy spectra of real discrete, crystalline systems [10]. It has also been used to embed imperceptible watermarks in image data [9, 15] and for motion detection in video sequences [16] (using the related "Mojette" digital projection transformation). Algorithms to perform efficient forward and inverse DRT transformation and for primitive translation and rotation in DRT space were presented in [11]. Because of its prime number basis, the DRT has strong links with number theory [8], to lattice properties through the Farey Series [18] and with the Riemann Hypothesis [10, 12].

2. DRT Overview

The DRT has its roots in the general, algebraic formalism for the projection of discrete m by n sets developed in [4] for seismographic applications, as the slant stack transformation. Adopting a p by p , prime-sized array [1], enabled the digital projections to be formed and inverted exactly using only addition of discrete values. That work also highlighted the group theory links of the DRT and its underlying Fourier relationships.

The use of straight-line digital projections to enhance oriented line data in images also has a long history as the Hough transform, a relative of the standard Radon transform. Recent work on exact 1:1 mappings for lines in discrete data [5] extends work on characterizing digital lines [2, 3].

A description of the properties of digital projections in the DRT can be found in [7, 10, and 14]. The DRT can also be applied to data on hexagonal arrays [6, 10]. A general discussion on connecting digitizations on hexagonal and square lattices is given in [17].

The DRT maps a 2D, p by p digital image, $I(x, y)$ to a 2D, p by $(p+1)$ space of digital projections, $R(t, m)$. The coordinates x , y , t , and m are all integers. The origin $(0, 0)$ of each space is arbitrarily set at the top left corner of the array. Each digital projection has p horizontal, integer-step translates, labelled by index t , with t ranging from 0 to $p - 1$. Each projection is associated with a unique angle in the data array, selected from a discrete set of $p + 1$ angles, labelled by index m , with m ranging from 0 to p .

The DRT forms the digital projection (t, m) by summing the contents of pixels located at $x = t$ on $y = 0$ and $x = t + m$ on $y = 1$ and so on, for $y < p$. The integer index m fixes, uniquely, the relative horizontal (x_m) and vertical (y_m) offset distances between nearest neighbor pixels along the digital rays for that projection. The offsets x_m and y_m are relatively prime integers. The angle of a digital ray, $\theta_m = \tan^{-1}(x_m/y_m)$, corresponds to the orientation of the line joining a pixel located on some digital ray (t, m) to its nearest ray neighbors for that same (t, m) . The nearest-neighbor distance between sampled pixels, measured along the digital ray direction, is $d_m^2 = x_m^2 + y_m^2$ for a square grid and $4d_m^2 = x_m^2 + 3y_m^2$ for a hexagonal grid (where the lattice horizontal and vertical spacing is $1/2$ and $\sqrt{3}/2$ units respectively). The set of digital projection angles θ_m is formed by integer ratios that have an approximately uniform distribution over the angle range 0 to π [10].

A point in an image $I(x, y)$ maps to a digital projection in $R(t, m)$ as

$$t = (x - my) \bmod(p) \quad (1)$$

$$m = (\alpha p + x_m) / y_m \quad (2)$$

for regular square arrays (where α is the smallest integer that makes m an integer), and for regular hexagonal arrays as

$$t = (x - (m + \frac{1}{2})y) \bmod(p) \quad (3)$$

$$m = (\alpha p + \frac{1}{2}(x_m - y_m)) / y_m \quad (4)$$

For a given m , all p translates of t form parallel digital rays. They each sample the data in the same pattern and with the same $x_m : y_m$ relative pixel offsets. When x_m is negative, we define $\pi/2 \leq \theta_m < \pi$. We chose 0 : 1 and 1 : 0 to represent projections taken along the row and column directions.

On a regular square array, a digital ray at $x_m : y_m$, has equivalent digital rays with integer ratios $-x_m : y_m$, $y_m : x_m$ and $-y_m : x_m$, generating full four-fold symmetry in the distribution of digital projection angles. For hexagonal arrays, the set of digital projection angles exhibits complete six-fold symmetry [14].

3. Local pixels and Digital Rays in the DRT

Each pixel at its location (x, y) in an image is projected along some digital ray with translate t for a given m value. On a square lattice, the neighbors of this pixel can be mapped to related t values, for digital rays of the same m value, using (1) and (2). The left and right immediate horizontal neighbors of a point in $I(x, y)$ will always correspond to digital rays at translates $t - 1$ and $t + 1$,

following the definition of unit translation in the DRT. The immediate vertical neighbors correspond to translates $t + m$ and $t - m$ for the points above and below the original data point because, by definition, points on adjacent rows have the same t value when they are m translate units apart. Using equation (1), labels for the digital ray passing through a location at a relative integer offset (i, j) from any given pixel location, on a square lattice, can be determined to be $t' = t + i - mj$. If $t' < 0$, or $t' \geq p$, the values are taken modulus p , so that the translate values for each m are treated as belonging to a circular buffer. By contrast, in continuous Radon space, pixel locations (x, y) are linked to the projection offset (ρ) and angle (θ) by $\rho = x \cos \theta + y \sin \theta$. For the DRT, the projection offsets are always integers.

All pixels are mapped to discrete translates in the DRT space. This enables local values from the 2D image space to be compared or combined using the corresponding translate values along each 1D digital projection. However it must be remembered that each entry in the DRT space is the sum of p values, one taken from each row of the image data. When accessing a local region of the image space via the DRT values for a given m value, the individual pixel contents are not available. A full image reconstruction, using the inverse DRT mapping, is required to obtain individual pixel values at any image location.

4. Lines in the DRT

The DRT samples the image data along digital ray directions at intervals of d_m . The presence of gaps between discrete samples is a marked point of difference with the continuous integrals of the Radon projection. The size of the DRT sample gaps scales as \sqrt{p} , so that for large reconstructed image sizes, the differences become less important and the DRT can be used, with little modification, to reconstruct images of high quality from real projection data [7].

By combining the digital rays at related translations for a given m value, it is possible to select pixels from the image array that have no gaps between them in the direction of the digital ray. Sampling image data along continuous, 4- or 8-connected periodic lines has representational advantages, particularly for orientation-sensitive, translation-invariant morphologic processing [13].

To form a continuous line at orientation $1 : m$, the sum of digital rays at translates t to $t + m - 1$ connects pixels with horizontal runs of length m . Connected periodic lines in the vertical direction correspond to digital rays at $t + \alpha m$, for integer α . Summed data values for pixels located along these connected lines can be accessed in the DRT data, for each m , by accessing the set of t values indicated above.

Figure 1 a) shows the pixels selected by the single digital ray for $m = 43$ and $t = 20$ for a 173 by 173 square array of pixels. Figure 1 b) shows 4-connected pixels at angle $-1 : 4$ selected by digital rays with $m = 43$, $t = 20 + \alpha m$, for integer α , $0 \leq \alpha \leq 3$, again for a square image of (prime) size 173. Figure 1 c) shows 8-connected pixels selected by the bundle of digital rays for $m = 43$, $t = 20$ to $20 + 42$ form periodic lines at an angle of $43 : 1$. Symmetric $1 : 4$ rays occur at $m = 4, 43, 130$ and 169 for $p = 173$.

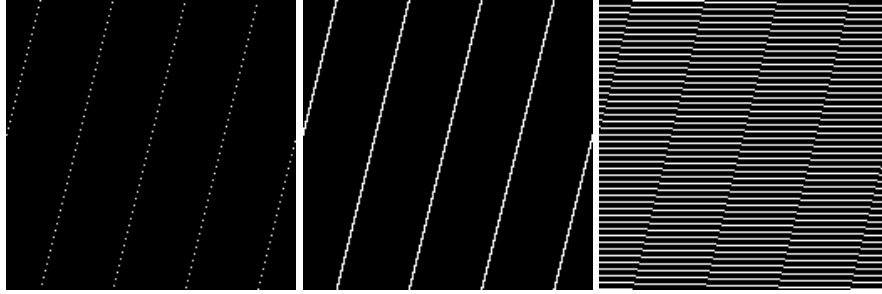


Figure 1. Digital rays and the formation of periodic lines on a 173 by 173 square array. (Left to right) a) Image pixels selected by the digital ray at $m = 43$, $t = 20$, b) image pixels selected by $m = 43$, $t = 20 + \alpha m$, for integer α , $0 \leq \alpha \leq 3$, c) image pixels selected by the bundle of digital rays corresponding to $m = 43$, $20 \leq t < (20 + 43)$.

The periodic lines require the pooling of several DRT projections to achieve line connectivity. To obtain vertical 8- or 4-connected line segments, only a selected set of m values wrap around the array of width p to fall one location left or right of that for the previous row (where $\alpha m \bmod(p) = \pm 1$). The set of connected lines able to be represented by bundles of digital rays is thus limited to the projections $x_m : y_m = 0 : 1$ and $1 : 1$, ranging up to $\pm 1 : y_{max}$ and $\pm y_{max} : 1$, where y_{max} is the maximum value of y_m for a given value of p . This subset of rays comprises $4y_{max} \approx 4\sqrt{p}$ angles from the full set of $p + 1$ digital angles [7]. The pooled digital projection values do not preserve an exactly invertible version of the original data. The original DRT needs to be retained if other processing is required.

5. Linear Operators

For linear operators, the summed image values stored at each (t, m) value in the DRT space creates several advantages. As the DRT is an exact, additive representation of the image data, the global variance of the original image data should be reflected through the variance of each of the digital projections.

The global variance of the data in any image $I(x, y)$, σ_I , can be expressed through the global variance, σ_R , in $R(t, m)$ by

$$\sigma_R = [p\sqrt{p}/(p + 1)]\sigma_I \quad (5)$$

The scale factor adjusts for the summation in R of p pixels from I for each translate at each projection angle. The variance is calculated for each of the $p + 1$ values of m in R and these values are combined as squares, representing independent contributions from each digital projection. This relationship enables the global image variance to be expressed directly in terms of the fractional variance contributed by each of the digital projections. Because the sum of squared values is calculated, it does not matter whether the variance is calculated before or after the image values have been summed. The vari-

ance preserving property of the DRT enables quantification of the information content contributed by each individual digital projection for any image.

The same invariance to the order of summation applies to the local convolution operator. The sum of values convolved in image space will be the same as the convolution of the summed values in DRT space. If G is a convolution operator and R is the DRT operation, then $R^{-1}GR = G$, where R^{-1} is the DRT inverse. The results of section 3 can be used to select those relative pixel offsets to define an arbitrary region of interest. Summing weighted pixel contents in $I(x, y)$ can be achieved in an exactly equivalent manner by summing the weighted contents at the appropriate translate positions of digital rays, for each m value in R .

Decomposing a convolution into a summation over single translated pixel locations is an inefficient means to process large connected regions of interest. Convolution using rows or products of row and column convolutions increases the processing efficiency for symmetric, decomposable weight distributions. The same efficiencies can be achieved in DRT space, as horizontally adjacent pixels are adjacent in DRT space. Vertically adjacent pixels can be accessed as points m steps apart along the translate axis. In such cases, greater efficiency can be achieved by rotating the whole image by rotating the digital projections, making use of the symmetry of the DRT space. Algorithms for rotating the image about the symmetry axes and for arbitrary integer translations of the image in DRT space are presented in [11]. For example, a $\pi/2$ rotation of image data on a square lattice is equivalent to mapping $R(t, m)$ to $R(t', m')$, where $m' = (\alpha p - 1)/m$ and $t' = m'(t + 1) \bmod(p)$.

The benefit of applying a convolution operation G in R space is that all of the multiply and accumulate steps can be done just using row data, for all rows. Faster memory access is possible if only p data points in a p by p image need to be fetched and cached. Each row of $R(t, m)$ can be processed independently. If multiple processors are available, each digital projection can be processed in parallel.

Figure 2 shows the result of a uniformly weighted, smoothing filter applied at one of the hexagonally symmetric angles. The initial image was a cropped, square image of "Lena" of size 479 pixels. The image was first mapped from a square to a hexagonal lattice and then digitally projected using the forward DRT. A $\pi/3$ rotation was applied to $R(t, m)$. The blurring was done on the hexagonal DRT data as a 15-pixel wide, horizontal uniform average of the DRT data for all m values, with the translates being treated as a circular buffer around $t = 0$ and $t = p - 1$. The blurred DRT data was rotated by $-\pi/3$ prior to inverse DRT transformation. The reconstructed data was then resampled from a hexagonal to a square lattice. The end result has had the original image subtracted from it, simply to emphasize the changes produced by the hexagonal filtering. Although the sequence of operations seems complex, only the inner DRT rotation, averaging and de-rotation operations need to be done for data stored and processed as (hexagonal) digital projections. These operations can be computed quickly and efficiently because of the 1D presentation of the data. The image content at the borders reflects the circular convolution used to perform the 1D averaging.



Figure 2. Changes in "Lena" produced by a 15-pixel wide blur at 60° , implemented in hexagonal DRT space (see text for details).

6. Non-linear Operators

The use of addition as the projection operation in the DRT means that all pixels in the image space are summed just once for all translations, $0 \leq t < p$, at each m value. The mean value of each row of $R(t, m)$ is thus the same for all m values and is equal to the total image brightness. A non-linear rule could also be used for projecting the pixel values along the digital rays. In this section, results are presented for maximum, minimum and median projected views along each of the digital rays.

Figure 3 shows the image reconstructed from digital projections of Lena where the value stored is the median of the p image values from $I(x, y)$ selected by each translation for the $p + 1$ values of m . The maximum and minimum reconstructed results correspond to upper and lower bounding objects. In the maximum projection, all rows of $R(t, m)$ have the same maximum value, equal to the global image maximum. In the minimum projection, all rows of $R(t, m)$ have the same minimum value, equal to the image minimum. As a result, although the reconstructed images show some fine spatial detail in the regions



Figure 3. Image reconstructed from the median intensity DRT digital projection of Lena.

around the locations of the extreme global values, the maximum and minimum DRT projections prove to be a blunt instrument.

The median projection values lie closer to the average value portrayed by the more usual summed DRT result. However, the median value of p image pixels over all (t, m) will generally have some variation with m that makes the reconstructed result an unbalanced combination of the digital projections. In the summed DRT, each projection sum is weighted uniformly. This enables each pixel value to be recovered exactly. The median value for a given t comes from one (or more) of many possible locations along the wrapped digital line segments, so that spatial connectivity of the projected result is not ensured. This produces the relatively flat and bimodal distribution of reconstructed image values seen in Figure 3.

Local erosion and dilation operators also require, as for convolution, pooled comparisons of the image data obtained from the discrete points that define a structuring element. Although the DRT enables access to the points that comprise a structuring element, the sum of local maximum values is not the same as the maximum of the local image sums. Hence performing morphologic filtering by direct calculation on the digital projections is a difficult as perform-

ing erosion and dilation operations on the Fourier transform of image data.

The pattern of pixel locations selected by each m value (for example, as shown in Fig. 1 a), can be thought of as constituting a uniquely shaped structuring element, but one that spans or wraps across the image space. The p horizontal translates of this structure at each projection does provide a 1D cyclic space in which 1D erosion and dilation can be defined, but only for the structuring elements that correspond to the pixel selection patterns for each m at a given prime, p .

7. Conclusions

This overview of the DRT has shown that transformation can simplify the algorithms for linear operations, because of the compression of 2D information into 1D digital projections. This same compression also makes it difficult to perform non-linear operations, as rank order does not commute with summation. Another difficulty with the DRT, as mentioned in [5], is the linking of parallel, but displaced digital line segments as the digital rays wrap around the array (with projection m wrapping $|x_m| + y_m$ times [7]). The wrapping of digital rays means that objects with a diameter d that is greater than the perpendicular distance between wrapped rays for a given t will intersect the same t more than once. The separation between wrapped rays is of order p/d_m . When $d > p/d_m$, the maximum projection at that m will have all translates intersecting this object at least once and hence the same maximum value is recorded at all translates. These m values will not contribute any contrast to the reconstructed image and the absence of projections at these angles will generate artifacts. These effects will be especially noticeable for binary image data.

The wrap problem may be avoided by storing, in a separate array, the projected values for each parallel line segment of a digital ray for each m . This would increase the storage capacity required for $R(t, m)$ (by around a factor of \sqrt{p}) and the algorithmic complexity to compute the partitioned DRT projections will be greater. The inverse algorithm, however, could still be computed relatively easily, as the DRT entries for each line segment at the same m value needs only to be summed over common t values to restore the original full DRT value and then the usual inverse algorithm can be applied.

Acknowledgments

Thanks to the Centre for X-Ray Physics and Imaging for providing support for this work.

References

- [1] F. Matus and J. Flusser. Image Representation via a Finite Radon Transform. *IEEE Transactions on Pattern Analysis and Machine Intelligence*, 15(10):996–1106, 1993.

- [2] J. Koplwitz, M. Lindenbaum and A. Bruckstein. The Number of Lines on a $N \times N$ Grid. *IEEE Trans. Information Theory*, 36(1):192–197, 1990.
- [3] I. Svalbe. Natural Representations for the Hough Transform. *IEEE Pattern Analysis and Machine Intelligence*, 12(2):336–342, 1991.
- [4] G. Beylkin. Discrete Radon Transform. *IEEE Trans. on Acoustics, Speech and Signal Processing*, ASSP-35(2):162–172, February 1987.
- [5] A. Averbuch, R. Coifman, D. Donoho, M. Israeli and J. Walden. Fast Slant Stack: A Notion of Radon Transform for Data in a Cartesian Grid which is Rapidly Computable, Algebraically Exact, Geometrically Faithful and Invertible. *TR No.2001-11*, www.stat.stanford.edu/research, May 2001.
- [6] P. Salzberg and R. Figueroa. Tomography on the 3D-Torus and Crystals. In G. T. Herman and A. Kuba, editors, *Discrete Tomography: Foundations, Algorithms and Applications*, Chapter 19. Birkhauser, Boston, 1999.
- [7] I. Svalbe and D. van der Spek. Reconstruction of Tomographic Images Using Analog Projections and the Digital Radon Transform. *Linear Algebra and its Applications*, 339:125–145, 2001.
- [8] J. Kung. Radon Transforms in Combinatorics and Lattice Theory. *Contemporary Mathematics*, 57:33–74, 1986.
- [9] I. Svalbe. *An Image Labelling Mechanism Using Digital Radon Projections*, ICIP, Thessalonika, Greece, 1015–1018, October, 2001.
- [10] I. Svalbe. *Digital Projections in Prime and Composite Arrays*, IWCIA, Philadelphia, August, 2001, also see Electronic Notes in Theoretical Computer Science, www.elsevier.nl/locate/entcs/volume46.free.
- [11] I. Svalbe. *Image Operations in Discrete Radon Space*, accepted for presentation, APRS, DICTA02, Melbourne, Australia, Jan. 21-22, 2002.
- [12] B. Klarrich. Prime Time. *New Scientist*, 168(2264):32–36, 2000.
- [13] R. Jones and P. Soille. Periodic Lines and Their Application to Granulometries, Mathematical Morphology and its Applications to Image and Signal Processing. P. Maragos, R. Schafer and M. Butt editors, pages 263–272. Academic Press 1996.
- [14] I. Svalbe. *Sampling Properties of the Discrete Radon Transform*, in review *Discrete Applied Mathematics*, 2001.
- [15] F. Autrusseau and J. V. Guedon. *Image Watermarking for Copyright Protection and Data Hiding via the Mojette Transform*, SPIE, Electronic Imaging, Conference no. 4675, Jan 21, 2002, <http://www.spie.org/Conferences/Programs/02/pw/ei.htm>.
- [16] F. Coudert, J. Benois-Pineau, P-Y Le Lan and D. Barba. *Binkey: A System for Video Content Analysis on the fly*, Proc. ICMCS, 1998, <http://www.computer.org/proceedings/icmcs/0253/Volumeno.201/0253967abs.htm>.
- [17] C. A. Wuthrich and P. Stucki. An Algorithmic Comparison between Square and Hexagonal-based Grids, Computer Vision. *Graphics and Image Processing: Graphical Models and Image Processing*, 53(4):324–339, 1991.
- [18] G. H. Hardy and E. M Wright *An Introduction to the Theory of Numbers*, Chapter 3, Oxford University Press, second edition, 1945.